Characterizing the Uncertainty in Holddown Post Load Measurements

J. A. Richardson
University of Alabama
Tuscaloosa, Alabama

J. S. Townsend
George C. Marshall Space Flight Center
Marshall Space Flight Center, Alabama

TABLE OF CONTENTS

LIST OF ILLUSTRATIONS

LIST OF TABLES

TECHNICAL PAPER

CHARACTERIZING THE UNCERTAINTY IN HOLDDOWN POST LOAD MEASUREMENTS

INTRODUCTION

History

The United States Space Transportation System (space shuttle) is an extremely complex system and demands rigorous engineering performance. For these reasons, along with safety concerns, it is very important that the engineer be able to accurately quantify the loads on the shuttle vehicle as well as the load uncertainties. Typically, loads are determined from engineering analyses and testing, with loads verification requiring special instrumentation of flight hardware.

The reaction forces at the shuttle vehicle/mobile launch platform (MLP) interface are considered in this study. A sketch of the lift-off configuration is given in figure 1. When positioned on the launch pad, the space shuttle is supported by eight posts, termed holddown posts (HDP's), which extend up from the MLP and attach to the aft skirts of the solid rocket boosters (SRB's). All shuttle external loading, such as main engine thrust, gravity, and wind, must react back to ground through these interfaces. Knowledge of these loads defines the design or limit load criteria of the SRB support skirt and the lift-off loads and dynamics that drive the shuttle primary structure and payload. The critical loads on the skirt occur during the approximately 7-s time period immediately prior to lift-off, when the space shuttle main engines (SSME's) are building up to maximum thrust. During a 1988 structural qualification test of a "modified" aft skirt, skirt post/skin welds failed at loads 1.28 times the critical loads. Because the desired factor of safety for the aft skirt was 1.40, and because SRB/MLP interface reaction loads verification has been a long-time engineering objective, NASA decided to measure the actual skirt loads during the SSME buildup phase of launch.

Commercially available load cells were not practical due to configuration constraints and the extremely large loads on the HDP's. Therefore, the HDP's themselves were instrumented with strain gauges and load calibrated, essentially making each HDP into a unique load cell. The HDP's were designed to be HDP's, however, and not load cells. Designing the instrumentation for the posts was difficult because the posts were unsymmetrical and very stiff (which meant very small strains).

NASA engineers were faced with many tough questions concerning the load cell design. How many strain gauges are necessary to measure the loads with sufficient accuracy? Where should the strain gauges be located so that all load components are measured accurately? What type of gauges should be used, shear or axial? Are the moment reaction loads significant, and to what extent do moments influence the accuracy of the shear loads measurements? Unfortunately, the engineers did not have quantitative information available at the time to help answer these questions. All load cell configuration decisions were based upon experimental trial and error testing of a multistrain gauged HDP. Recently, quantitative information was generated by the authors using simple probabilistic techniques. The probabilistic techniques were directed to answer specific questions posed by the co-author, a NASA engineer thoroughly familiar with the history and problems of the HDP load cells.

Load Cell Configuration

A closeup view of a typical HDP/aft skirt interface is shown in figure 1. The structural components that make up the interface are the skirt foot (post), the skirt shoe, the epon shim, the spherical bearing, and the MLP HDP. Note also, that a pretensioned holddown stud is used to sandwich these components together. Although the load path is not simple, all loads must react through the MLP post, making it the prime candidate for the structural load cell. Figure 2 shows a typical HDP mounted to the MLP at Kennedy Space Center.

The strain gauge transducers for the HDP load cell are located on the inside of the post. Eight strain gauge clusters are positioned in a single ring around the inner circumference of the HDP at a distance of about 28 in from the top of the post. Each cluster consists of four axial gauges arranged to compensate for temperature and poisson effects and to amplify output sensitivity. Shear gauge transducers are also positioned on the posts, but, because of extremely low output, these gauges have proven to be of little practical use. As mentioned previously, the current HDP load cell configuration was based on findings from experimental testing. At the time, the frictional moment constraint was assumed to be a second-order effect and was ignored (the moment was assumed to be zero at the top of the post). Additional testing, however, later indicated that the moment effects are not negligible. Recently, a new post load cell has been designed, tested, and flight implemented to measure both shear and moment loads. The accuracy of this "improved" load cell is also in question.

Typical HDP load histories from eight flights are shown in figure 3. As seen in the figure, the vertical (x direction) loads do not deviate much, percentage wise, from flight to flight. The horizontal loads, however, deviate significantly from flight to flight. This scatter in data may represent actual deviations in the HDP loads from flight to flight, or may be due to measurement error. The z-direction loads do not satisfy equilibrium checks, however, indicating that the z-load variation is due (at least partly) to measurement error.

A two-step procedure is followed to calculate stresses in the aft skirt from measured HDP strains. In this procedure, diagrammed in figure 4, the HDP strains are multiplied by a calibration matrix to yield HDP loads. The HDP loads are then multiplied by aft skirt stress indicator equations to yield the aft skirt stresses. An HDP is calibrated by removing it from the MLP and bolting it to a test stand. Controlled loads are then applied to the HDP, and the resulting strains are measured. The measured strains and loads are used to form a matrix of calibration constants for that post.

The effect of strain measurement errors and calibration constant errors on the accuracy of the HDP load measurements is examined in the next section. The x loads are shown to be the most sensitive (have the largest standard deviation) to strain measurement and calibration constant errors in an absolute sense. However, the z loads are the most sensitive in a relative sense (largest standard deviation/mean), which agrees with the actual load histories shown in figure 3. The deviation in HDP loads caused by strain measurement and calibration constant errors seriously affects the accuracy of the predicted aft-skirt stresses, as shown in the following section.

ACCURACY OF HDP LOAD MEASUREMENTS

A simple probabilistic analysis technique, Monte Carlo simulation, was used to investigate the effect of known sources of error on the HDP load measurements. A schematic diagram of the procedure

for investigating the effects of strain measurement errors is shown in figure 5. Each of the eight strain measurements was assumed to vary about its mean within a range of ± deviation. This deviation represented the difference or error between the true HDP strains and the measured HDP strains. Since no actual data on the HDP strain measurement errors were available, these errors were modeled with the simplest probability distribution: the uniform distribution. In a uniform distribution, the values have an equal probability of occurrence within the range: (mean – deviation) to (mean + deviation).

A set of three HDP loads (Px, Py, and Pz in fig. 5) was calculated by drawing a strain measurement at random from each of the eight strain probability distributions and multiplying by the calibration matrix. This procedure was repeated 1,000 times to produce the HDP-load probability distributions. The HDP-load distributions resembled bell-shaped or normal probability distributions. The measure of dispersion for these distributions is the standard deviation. The standard deviation can be normalized by dividing by the mean of the distribution to yield the coefficient of variation (COV).

Effect of Strain Variations on HDP Loads

Since the peak stresses in the aft skirt occur when the HDP loads are at their peak values, (approximately 1.2 s before separation in fig. 3), the measured strains from a typical flight at 1.2 s before separation were used as the mean strains for the strain distributions. The mean strains and mean loads used for the simulation are shown in table 1. As mentioned, no data on the actual strain measurement errors were available. A practical lower bound on strain measurement errors is ±5 microstrains (strain $\times 10^{-6}$). Strain measurement errors are more likely in the range of ±10 microstrains.

HDP load distributions were generated for strain deviations of ±0, 1, 2, ... 10 microstrains. The standard deviations of the x, y, and z loads for each strain deviation are plotted in figure 6. The x loads are twice as sensitive to strain deviations as either the y or the z loads. However, on a relative basis, the z loads are approximately two times more sensitive to strain variations as the y loads, and four times more sensitive than the x loads, as shown in table 2.

The reason the x loads are most sensitive (on an absolute basis) to strain variations is the strains produced by a unit x load are approximately half the strains produced by either y or z loads, as shown in the next section.

Effect of Calibration Constant Variations on HDP Loads

The HDP's were calibrated by mounting each post in a test rig and applying measured loads in one direction only. Typical strain measurements at each of the eight gauges from a calibration procedure are shown in table 3. These strains are the calibration constants for one HDP. The 8 by 3 matrix of calibration constants (A) was manipulated to produce the calibration matrix (C) as follows.

$$C = [A^T A]^{-1} A^T . \tag{1}$$

The calibration matrix C multiplied by the strain measurements equals the HDP loads.

To study the sensitivity of the HDP loads to deviations in individual calibration constants, a single calibration constant was allowed to vary within ±0.01 of its mean, while the other calibration constants remained constant. The calibration matrix (C) was then calculated and multiplied by the mean

strains from table 1. The procedure was repeated for each of the 24 calibration constants in table 3. The results, presented in figure 7, show that not only the x loads, but also the y and z loads, are most affected by variations in the x calibration constants. This implies that insensitivity to one load direction affects the sensitivity to the other load directions for this load cell. The average strain magnitude of the x-load calibration constants is approximately half the average strain magnitude of the y and z-load calibration constants.

The effect on HDP loads of simultaneous variations in strain measurements and variations in calibration constants was studied by performing three sets of simulation runs. In the first set, the calibration constant deviations were set equal to zero. In the second set, the calibration constant deviations were set equal to their minimum values based on the results of the calibration tests. In the third set, the calibration constant deviations were set equal to higher but still realistic values. Uniform probability distributions were used to model the calibration constant variation.

An example showing the calibration constant deviations from a test on a single HDP is shown in figure 8. A total of 14 tests were completed for each strain gauge to determine the X-calibration constants. The tests included both $+X$ and $-X$ axial loading with the HDP oriented in six different horizontal positions relative to the test fixture base. Each test configuration requires that the HDP be unbolted from the pedestal, reoriented, and then rebolted. Data scatter is attributed to slight differences in the position of the HDP relative to the test fixture pedestal (due to bolt-hole tolerances between the post and the pedestal). Also, data scatter occurred during the $+X$ and $-X$ axial load tests of a given configuration. In this case, data scatter results from slightly different load paths between tension $(+X)$ and compression $(-X)$ loading. Tension loads react from the bottom of the stud/post nut interface, while compression loads react into the post through the spherical bearing (fig. 1). The X-calibration factor was determined by averaging the 14 test values to give a single deterministic value. The Y- and Z-calibration constants were determined in a similar manner as X, but fewer tests per configuration were examined.

In the STS flight configuration, the HDP is bolted to a similar pedestal mounted on the MLP. Since the HDP's were calibrated independent of the MLP pedestal and then bolted into position, the "true" calibration constants for a given post are slightly different than those determined during the calibration tests. Based on abundant calibration data, as well as the extensive personal experience of the co-author, the deviations listed in table 4 were chosen for the minimum and the high calibration constant deviations.

The results of the 33 simulation runs are shown in figure 9. In this figure, the standard deviations of the HDP loads are plotted separately but to the same scale for the x, y, and z loads. As expected, the x loads are more affected by the calibration constant deviations than either the y or the z loads. The figure also shows that strain deviations have little effect when calibration constant deviations exist.

Effect of HDP Load Deviations on Aft-Skirt Stresses

The trends have been identified for the effect of strain and calibration constant deviations on HDP load deviations. The implications for the predicted aft-skirt stresses were investigated by constructing two representative sets of load distributions. For the first set (load case 1), minimum strain and calibration constant deviations were used. Higher but realistic strain and calibration constant deviations were used to construct the second set of load distributions (load case 2). The strain and calibration constant deviations for each load case are listed in the first column of table 5. The resulting load distributions are plotted in figure 10; their standard deviations and COV are listed in table 5.

4

The procedure for calculating aft-skirt stresses from HDP loads is shown in figure 11 . The aft skirt is supported on four HDP's, each having an x, y, and z load component. The 12 HDP loads are premultiplied by a 4 by 12 matrix of stress indicator coefficients to yield four stresses. Each stress is located in the critical weld region above an HDP. Typical peak HDP loads during the buildup of the main engine were used as the mean values for the load distributions. The loads are listed in table 6.

The stress indicator coefficients used to calculate the stress above HDP No. 8 (for the left skirt) are listed below.

$$\text{Stress above HDP No. 8} = \begin{matrix} -0.650P_x^5 & +0.324P_y^5 & +0.921P_z^5 \\ -0.420P_x^6 & 0.350P_y^6 & +1.414P_z^6 \\ +1.900P_x^7 & -3.139P_y^7 & +3.037P_z^7 \\ -11.00P_x^8 & -5.556P_y^8 & -27.62P_z^8 \end{matrix} \quad (2)$$

The subscripts denote the direction of the load, and the superscripts denote the HDP number (the left skirt is supported on post Nos. 5 through 8). Note that the predicted skirt stress is most sensitive to the z load of post No. 8.

The results from the two simulation runs (shown in fig. 12) indicate that even with the minimum strain and calibration constant deviations, the predicted aft-skirt stresses are scattered over a 12-ksi range. When the strain and calibration deviations are doubled, the predicted skirt stresses are scattered over a 24-ksi range. The bar chart in figure 13 identifies the x-load deviation as the greatest contributor to the scatter in the predicted skirt stress. Figure 7 supports this finding. The uncertainty in the skirt weld stress is verified using the flight measured data plotted in figure 14.

Figure 14 graphs the predicted aft-skirt stresses (CWSI) verses the measured skirt strains in the critical weld region. The predicted stress values are based on the measured HDP loads and critical weld stress indicator equations (equation (2)). Data from 18 STS flights are plotted, as well as critical strains for compression posts 3, 4, 7 and 8. The data values correspond to aft-skirt weld peak stresses and strains at 1.2 s just prior to launch. The dash curve defines the expected relationship between the aft-skirt compression post strains and the critical weld stress. This curve was determined from a detailed math model of the skirt and verified through testing. Notice, for a given strain value, the CWSI predicted values are much higher than expected. If the CWSI equation is assumed to be accurate, and the measured strain values define minimum uncertainty, then the load predictions must be in error. Two errors are noted. First, the offset distance between the expected and actual median stress curves indicates a gross measurement error in the loads (corresponding to about 15 ksi). It is believed that this result is due to a moment load at the MLP post-spherical bearing/aft-skirt shoe interface (both the math model and test verification method assumed a zero interface moment). Second, scatter in the predicted skirt stress data about the actual median CWSI-strain curve is similar to the data scatter identified previously in figure 12. This result implies that the uncertainty in the measured loads is in part due to strain measurement error and calibration constant error. Furthermore, if the moment load was measured with minimal scatter and the actual and expected median curves then overlapped, a CWSI scatter range of 15 ksi is still expected.

The findings indicate that the measured HDP loads cannot reliably predict aft-skirt stresses. The principle reason behind the inadequacy of the load cells is the errors in the x calibration constants (second column of table 3). Errors in the x calibration constants affect not only x-load predictions

5

but y and z loads as well. The x-calibration constants are susceptible to errors because they are small numbers. As shown in the next section, x strains, and therefore the x-calibration constants, can be increased only by decreasing the axial area of the HDP.

EVALUATION OF HOLDDOWN POST AS A LOAD CELL

The instrumented HDP's were shown to be flawed load cells in the previous section. This section presents the effects on the HDP loads of changing the load cell geometry. For this purpose, the HDP load cell is modeled as a simple cantilever beam with two strain gauges, as shown in figure 15. The height from the top of the post to the strain gauges is 28 inches in the actual HDP and the posts are approximately 20-in wide at that height. The modulus of elasticity was arbitrarily assumed to be 30,000 ksi. The cross-sectional area and the moment of inertia of the cantilever model were calculated so that typical peak loads would cause typical strains. The typical loads and strains shown in table 1 were used. Gauges Nos. 1 and 2 in the cantilever model represent gauges Nos. 1 and 5, respectively, in the actual post. The mean loads, strains, and cross section properties are summarized in table 7. The equation relating strains to loads is shown below.

$$
\left\{ \begin{array}{c} \varepsilon_1 \\ \varepsilon_2 \end{array} \right\} = \left[\begin{array}{cc} \dfrac{-1}{EA} & \dfrac{-hw}{2EI} \\ \dfrac{-1}{EA} & \dfrac{hw}{2EI} \end{array} \right] \left\{ \begin{array}{c} P_x \\ P_z \end{array} \right\} .
$$

(3)

Effect of Load-Point Deviations on HDP Loads

The effects of deviations in the load point on the measured HDP loads were studied. When the HDP's are calibrated, the vertical load is applied in the center of the post. During assembly of the shuttle vehicle, however, the vertical load point is sometimes slightly off center due to a mismatch between the MLP HDP's and the SRB aft skirts. The bearings in the top of the HDP's are built to accommodate the slight mismatch, and actual load points can vary by ±0.25 in for a shuttle flight.

Two Monte Carlo simulation runs were performed in which the vertical load point was allowed to vary uniformly about the center of the post by ±0.25 in and by ±0.50 in. The strains were allowed to vary simultaneously. For each iteration of the simulation, a pair of strains (ε_1 and ε_2) and a load-point deviation (δ) were drawn at random. The calibration constants were then recalculated as shown in equation (4). The calibration matrix (C) was recalculated using equation (1) and, finally, the loads P_x and P_z were calculated.

$$
\left\{ \begin{array}{c} \varepsilon_1 \\ \varepsilon_2 \end{array} \right\} = \left[\begin{array}{cc} \dfrac{-1}{EA} - \dfrac{\delta w}{2EI} & \dfrac{-hw}{2EI} \\ \dfrac{-1}{EA} + \dfrac{\delta w}{2EI} & \dfrac{hw}{2EI} \end{array} \right] \left\{ \begin{array}{c} P_x \\ P_z \end{array} \right\} .
$$

(4)

The simulation results, shown in figure 16, indicate that the x load is not affected by load-point deviations. The z loads, however, were affected by the load-point deviations. Interestingly, simultaneous strain and load-point deviations were not linearly additive. For example, doubling the strain and load point deviations does not quadruple the z-load deviation.

Effect of Gauge Height on HDP Loads

The effect of moving the strain gauges higher and lower on the HDP was studied next. At each new height (h), new mean strains were first calculated by multiplying the mean loads in table 7 by the recalculated calibration constants shown in equation (3). The calibration constants then remained constant throughout the simulation. The procedure was repeated for each height.

As shown in figure 17, the standard deviation of the x load was not affected by changing the gauge heights while the z loads were affected. As the gauges were moved farther down the post, the strains caused by the same z load increased. These larger strains were less affected by strain deviations, resulting in less z-load deviation. Considering gauge height only, prediction of z loads would be improved (made less sensitive to strain deviations) if the gauges were located as low on the post as possible.

Effect of Number of Gauges on HDP Loads

In order to study how moment HDP loads were affected by strain deviations, two gauges were added to the cantilever model 18 in below the top of the post. A second set of eight gauges has been added to the actual MLP HDP's at this location for the purpose of separating moment and horizontal load effects. Adding additional strain measurements to the cantilever model tended to decrease the HDP load deviations, except in one case, as explained below.

The standard deviations of x, z, and moment HDP loads for several gauge configurations are shown in table 8. The strain deviation was set at a constant ±10 microstrains for all calculations for this table. In the first configuration, two gauges are located 28 in below the top of the HDP. The standard deviations for this configuration are shown in the first row of table 8. The equations for P_x and P_z for a post instrumented with two gauges only are given below.

$$P_x = -\frac{EA}{2}\left(\varepsilon_1 + \varepsilon_2\right) , \tag{5}$$

$$P_z = -\frac{EI}{w}\left(\frac{\varepsilon_1 - \varepsilon_2}{h}\right) . \tag{6}$$

When the two gauges are moved up to 18 in below the top of the post, the x-load deviation remains constant while the z-load deviation increases. The increase in the z-load deviation is directly proportional to the decrease in gauge height (h).

$$\frac{24.7}{15.9} = 1.55, \qquad \frac{1/18\ inches}{1/28\ inches} = 1.55 .$$

7

When four instead of two gauges are used, and the measurement system is calibrated to measure P_x and P_z only (not moment), both the x-load and the z-load deviations decrease, as shown in the third row of table 8. The equations for P_x and P_z for this strain-gauge configuration are shown below. The deviation of the sum of the (random strain) distributions is less than the sum of deviations of each distribution.

$$P_x = -\frac{EA}{4}\left(\mathcal{E}_1 + \mathcal{E}_2 + \mathcal{E}_3 + \mathcal{E}_4\right),\qquad (7)$$

$$P_z = -\frac{EI}{w}\left(\frac{\left(\mathcal{E}_1 - \mathcal{E}_2\right) + \left(\mathcal{E}_3 - \mathcal{E}_4\right)}{h_{1,2} + h_{3,4}}\right).\qquad (8)$$

If the four-gauge measurement system is now calibrated to measure P_x, P_z, and M_y, the x-load deviation remains the same, but the z-load deviation increases dramatically. The equations for P_x, P_z, and M_y are shown below. The equation for P_x remains the same as when the post is calibrated for P_x and P_z only. However, the denominator of the equation for P_z has now changed.

$$P_x = -\frac{EA}{4}\left(\mathcal{E}_1 + \mathcal{E}_2 + \mathcal{E}_3 + \mathcal{E}_4\right),\qquad (9)$$

$$P_z = -\frac{EI}{w}\left(\frac{\left(\mathcal{E}_1 - \mathcal{E}_2\right) - \left(\mathcal{E}_3 - \mathcal{E}_4\right)}{h_{1,2} - h_{3,4}}\right),\qquad (10)$$

$$M_y = -\frac{EI}{w}\left(\frac{h_{3,4}\left(\mathcal{E}_1 - \mathcal{E}_2\right) - h_{1,2}\left(\mathcal{E}_3 - \mathcal{E}_4\right)}{h_{3,4} - h_{1,2}}\right).\qquad (11)$$

The increase in the z-load deviation is directly proportional to the change in the denominator from equation (8) to equation (10).

$$\frac{\dfrac{1}{28''+18''}}{\dfrac{1}{28''-18''}} = 4.60,\qquad \frac{62.9}{13.7} = 4.59.$$

The effect on the x, z, and moment load deviations of moving the second set of gauges up and down the post (while the first set remains at a height of 28 in) is shown in figure 18. It is the distance between the first and second set of gauges, rather than the height of the gauges, which controls the shear and moment deviations. The greater the separation between gauges, the lesser the load deviations. If the second set of gauges is located at the top of the post ($h_{3,4} = 0$), then equation (11) reduces to the following.

$$M_y = -\frac{EI}{w}\left(\frac{\left(\mathcal{E}_3 - \mathcal{E}_4\right)}{1}\right).\qquad (12)$$

8

This equation for M_y is similar to equation (6) for P_z. The ratio of the standard deviation of M_y to the standard deviation of P_z equals 28, which is equal to $h_{1,2}$. The moment deviations will always be 28 times larger than the z-load deviations (for this case). This is because the strains caused by a z load are multiplied by the distance from the load point to the gauges (h). Larger strains are less affected by strain deviations. This implies that in the actual HDP's, strain deviations will cause larger deviations in the moment measurements than in the z-load measurements.

Effect of HDP Area and Moment of Inertia

Equation (7) indicates that the sensitivity of the axial HDP loads to strain deviations can be decreased by reducing the axial area of the HDP. This trend is also indicated in figure 19, which in addition shows that shear and moment load deviations are not affected by changing the axial area of the post. Reducing the moment of inertia of the posts decreases the sensitivity of the shear and moment loads to strain deviations (fig. 20), but does not affect the axial loads.

CONCLUSIONS

(1) Simulation studies indicate that the instrumented HDP's are sensitive to small strain deviations and to typical calibration constant deviations. The minimum load deviations are approximately ±35 kips for x loads and ±20 kips for y and z loads. (These numbers represent ± two standard deviations.) Higher but not unrealistic load deviations are approximately ±70 kips for x loads and ±40 kips for y and z loads.

(2) During calibration, the x-load strains are smaller than the strains caused by equal magnitude y or z loads. These smaller x-load strains are more susceptible to deviations (errors) in strain measurements and calibration procedures. When used as calibration constants, the x-load strains affect the dispersion of not only the x loads, but of the y and z loads as well.

(3) The dispersion in the HDP loads causes deviations in the predicted aft-skirt stresses. Minimum deviation of the predicted skirt stresses is approximately ±6 ksi (± two standard deviations), while higher but realistic stress deviation is approximately ±14 ksi.

(4) Simulation studies on a simple cantilever-post model of the HDP measurement system indicate the following.

    (a) Vertical load-point deviations do not affect the x loads but do cause z-load deviations. Realistic vertical load point deviations of ±0.25 inches cause z-load deviations of from 10 to 40 percent of the deviations caused by strain measurement errors.

    (b) Adding more strain gauges decreases the dispersion of the x and z loads due to a property of the summation of random distributions.

    (c) The dispersion of the z loads increased fourfold when the measurement system was calibrated for x, z, and moment loads, as compared to when it was calibrated for x and z load only.

    (d) Increasing the separation between the two sets of HDP strain gauges decreases the effect of strain deviations on the z and moment HDP loads.

(e)   Strain deviations will always cause larger moment deviations than shear deviations because the actual strains caused by shear loads are magnified by the distance from the load point to the gauges.

(f)   The x-load deviations can be decreased by decreasing the axial area of the HDP's, while z and moment load variations can be decreased by decreasing the moment of inertia of the HDP's.

(5)   One possible way to improve the accuracy of the HDP load cells without adversely affecting the skirt is to decrease the axial area of a section of each HDP while keeping the moment of inertia constant. This would increase the axial strains, which would increase the x-load calibration constants, which, in turn, would decrease the dispersion of the x, y, and z loads.

REFERENCES

1. Moore, N.R., Ebbeler, D.H., Newlin, L.E., Sutharshana, S., and Creager, M.: "An Improved Approach for Flight Readiness Certification—Methodology for Failure Risk Assessment and Application Examples." Jet Propulsion Laboratory Report under NASA RTOP 553-02-01, May 1992.

2. DeHoff, E.A.: "Solid Rocket Booster Holddown Post Calibration Testing." Report by Lockheed Engineering and Sciences Company, NASA contract 17900, Structures and Mechanics Division, September 1989.

3. Wiersma, H.: "MLP Bushing Rotation Anomaly." Report by United Technologies, USBI-1254-100, February 1990.

4. Mann, B.A., and Dell, L.P.: "Analytical/Measured Prelaunch HDP FRR Baseline Loads." Presentation at the Loads Panel by Rockwell International, February 1990.

5. DeHoff, E.A.: "Solid Rocket Booster Holddown Post Loads Reconstruction." Report by Lockheed Engineering and Sciences Company, No. SMD-90-1244/LESC 28204, April 1990.

Table 1. Base values for HDP loads and strains for eight-gauge model.

Mean Loads		Mean Strains	
Load Component	Load (kips)	Gauge No.	Strain (Microstrains)
Px	1,238	1	−84.6
Py	391	2	−136.0
Pz	-163	3	−239.2
		4	−276.8
		5	−191.6
		6	−108.0
		7	48.2
		8	−39.4

Table 2. *X*, *Y*, and *Z* HDP load deviations versus strain deviations.

Strain Deviation (Microstrains)	*Px*		*Py*		*Pz*	
	Std. Dev. (kips)	abs(COV) (Percent)	Std. Dev. (kips)	abs(COV) (Percent)	Std. Dev. (kips)	abs(COV) (Percent)
0	0	0	0	0	0	0
2	3.9710	0.32	1.9240	0.49	1.9570	1.20
4	7.9770	0.64	3.9710	1.02	3.9660	2.44
6	12.1500	0.98	5.9560	1.52	5.9020	3.63
8	16.3500	1.32	8.0050	2.05	8.1140	4.99
10	19.7700	1.60	10.0700	2.58	10.2500	6.30

Table 3. HDP calibration constants.

Strain Gauge	Unit Strains (Microstrains /kip)		
	X-Direction only	*Y*-Direction only	*Z*-Direction only
1	−0.1023	0.0585	−0.3220
2	−0.1041	−0.1829	−0.2032
3	−0.0836	−0.2813	0.0538
4	−0.1147	−0.2881	0.2558
5	−0.0927	−0.0080	0.2401
6	−0.0952	0.2029	0.1607
7	−0.1055	0.2502	0.0292
8	−0.1063	0.2076	−0.2023

Table 4. Calibration constant deviations used for simulation runs.

	X Load Constants	Y Load Constants	Z Load Constants
minimum	±0.005	±0.01	±0.01
high	±0.01	±0.02	±0.02

Table 5. Two HDP load distributions.

Strain Deviation (Microstrains)	P_x		P_y		P_z	
	Std. Dev. (kips)	abs (COV) (Percent)	Std. Dev. (kips)	abs (COV) (Percent)	Std. Dev. (kips)	abs (COV) (Percent)
Load Case 1 (minimum errors) strain dev. = ±5 microstrains X cal. con. = ±0.005 Y cal. con. = ±0.01 Z cal. con. = ±0.01	18.6	1.5	9.4	2.4	9.4	5.8
Load Case 2 (high errors) strain dev. = ±10 microstrains X cal. con. = ±0.01 Y cal. con. = ±0.02 Z cal. con. = ±0.02	38.6	3.1	19.0	4.9	19.2	11.9

Table 6. HDP mean loads used to calculate skirt stress distributions.

HDP No.	Load Direction	Mean Load, kips
5	X	–440
	Y	51
	Z	61
6	X	–440
	Y	–100
	Z	88
7	X	1,120
	Y	–260
	Z	–300
8	X	1,310
	Y	285
	Z	–215

Table 7. Base values for HDP loads and strains for cantilever model.

Mean Loads		Mean Strains		Cantilever Properties	
Load Component	Load (kips)	Gauge No.	Strain (micro-strains)		
Px	1,238	1	–84.6	Gauge Height (h)	28 in
Pz	–163	2	–191.6	Width (w)	20 in
				Modulus (E)	30,000 ksi
				Area (A)	299 in^2
				Moment of Inertia (I)	28,465 in^4

Table 8. Effect on HDP loads of number of gauges and whether post is calibrated for moment or not. Strain deviation = ±10 microstrains.

HDP Model	Standard Deviation, kips		
	Px	Pz	My
2 gauge, h = 28 in	36.6	15.9	—
2 gauge, h = 18 in	36.6	24.7	—
4 gauge, h = 18 and 28 in, calibrated for zero moment	25.7	13.7	—
4 gauge, h = 18 and 28 in, calibrated for moment	25.7	62.9	1,480

14
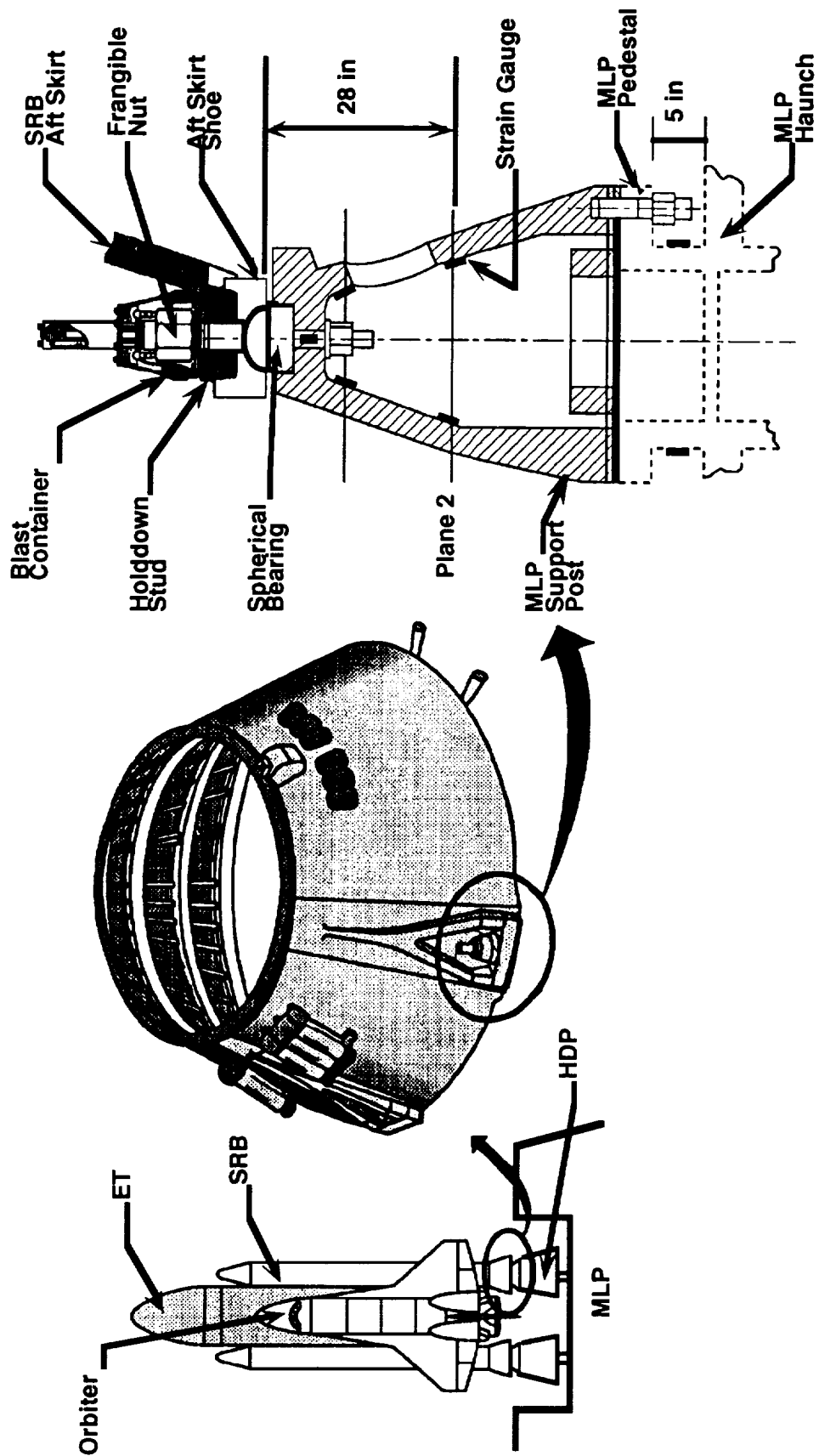
Figure 1. SRB aft skirt/MLP HDP interface.
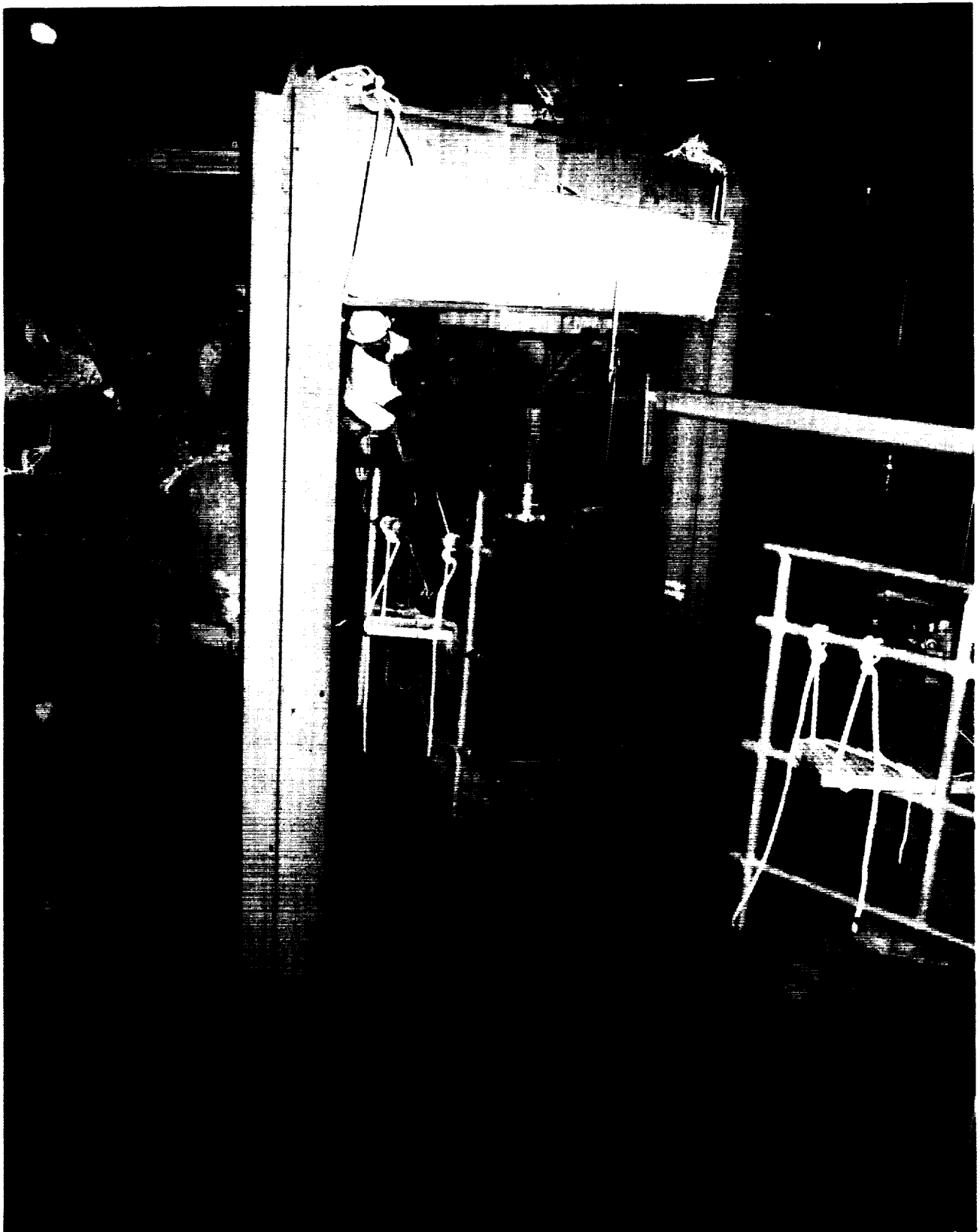
Figure 2. HDP mounted to MLP.

16
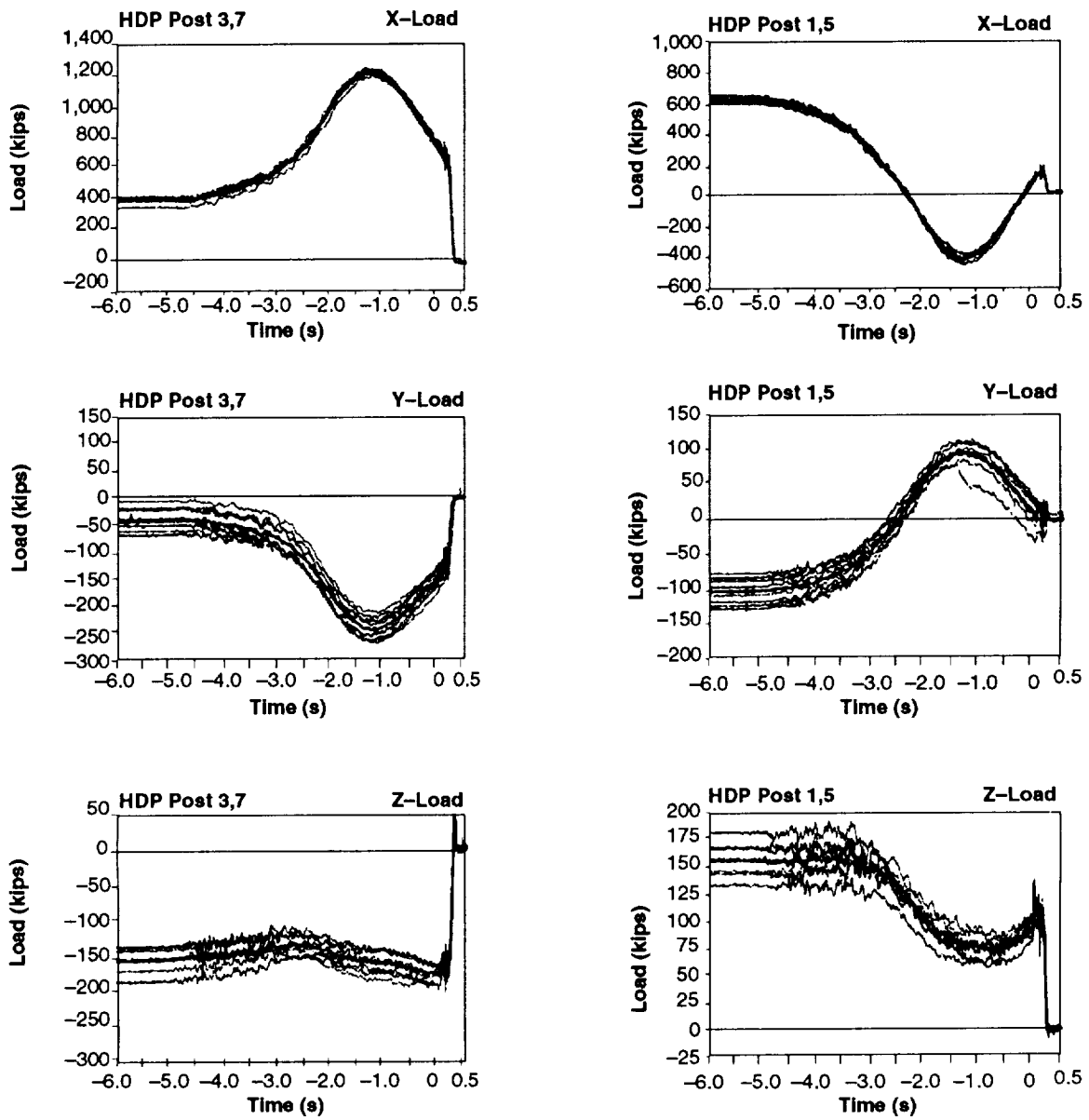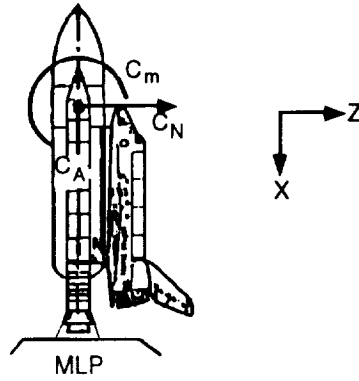
Figure 3. HDP load histories.
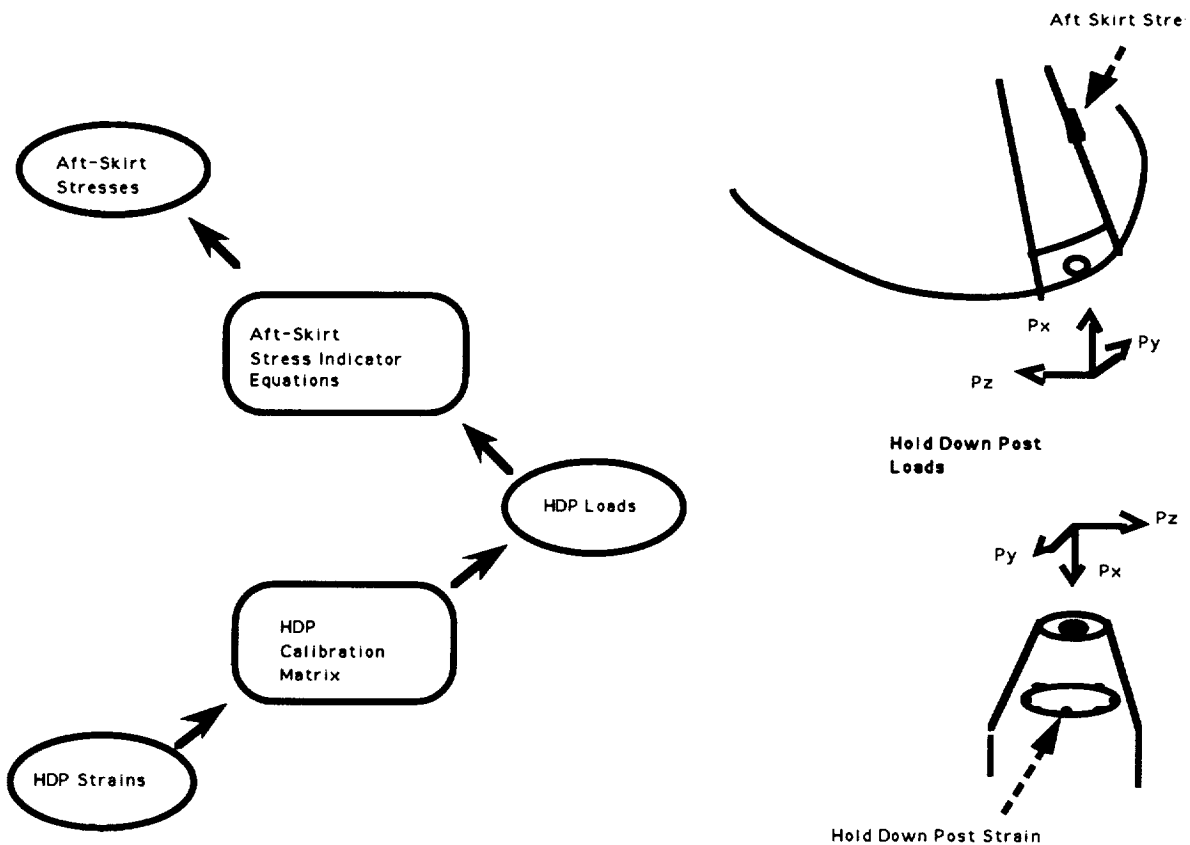
Figure 4. Procedure for calculating aft-skirt stresses from measured HDP strains.
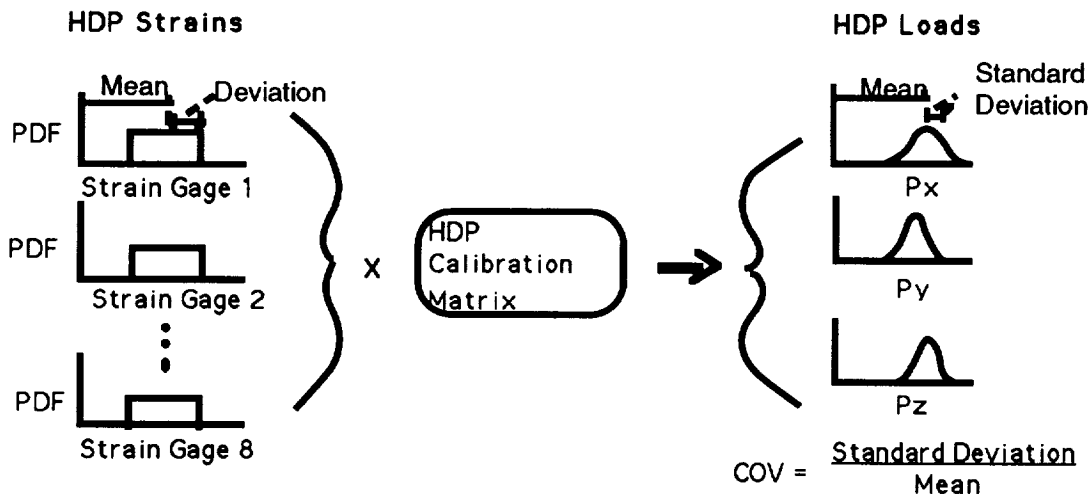
Figure 5. Procedure for calculating HDP load distributions from HDP strain distributions.
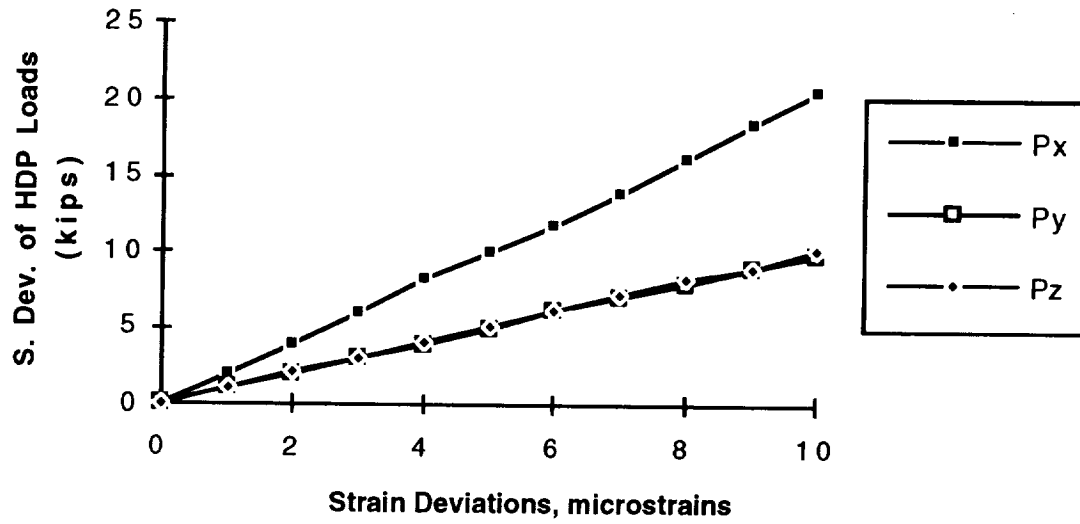
Figure 6. Effect of strain deviation on *X*, *Y*, and *Z* HDP load deviations.
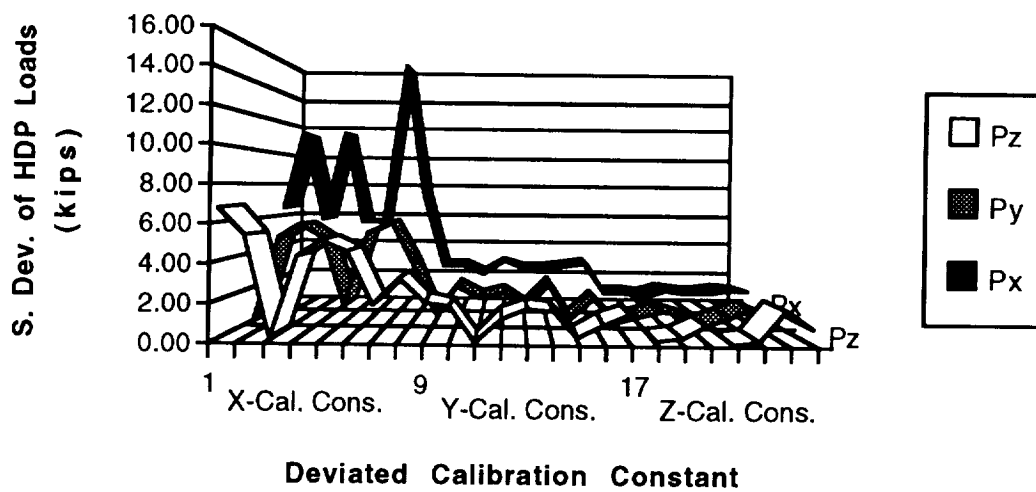
Figure 7. Sensitivity of HDP loads to individual calibration constant deviations of ±0.01.
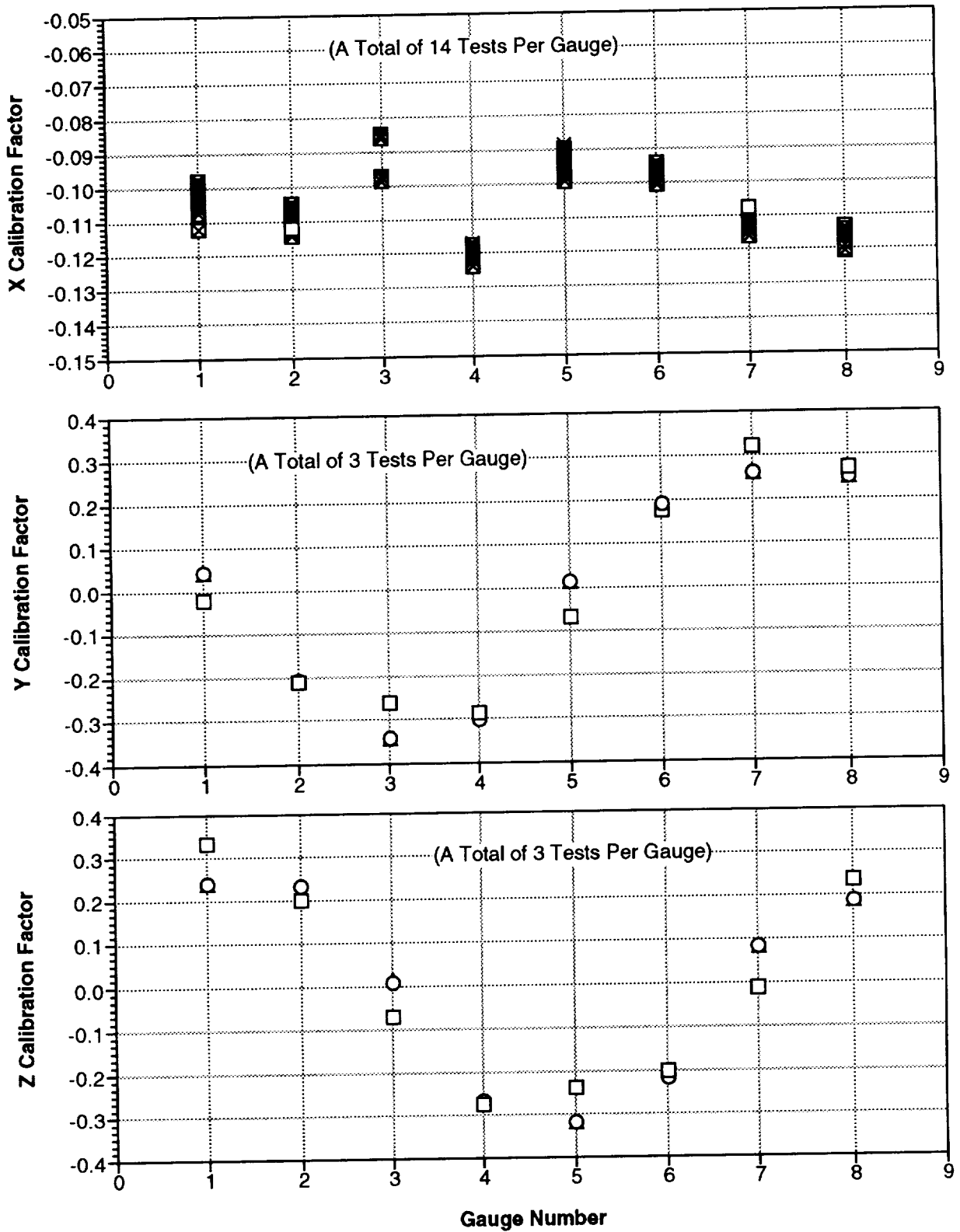
Figure 8. Test results for *x, y,* and *z* calibration constants for a single HDP.
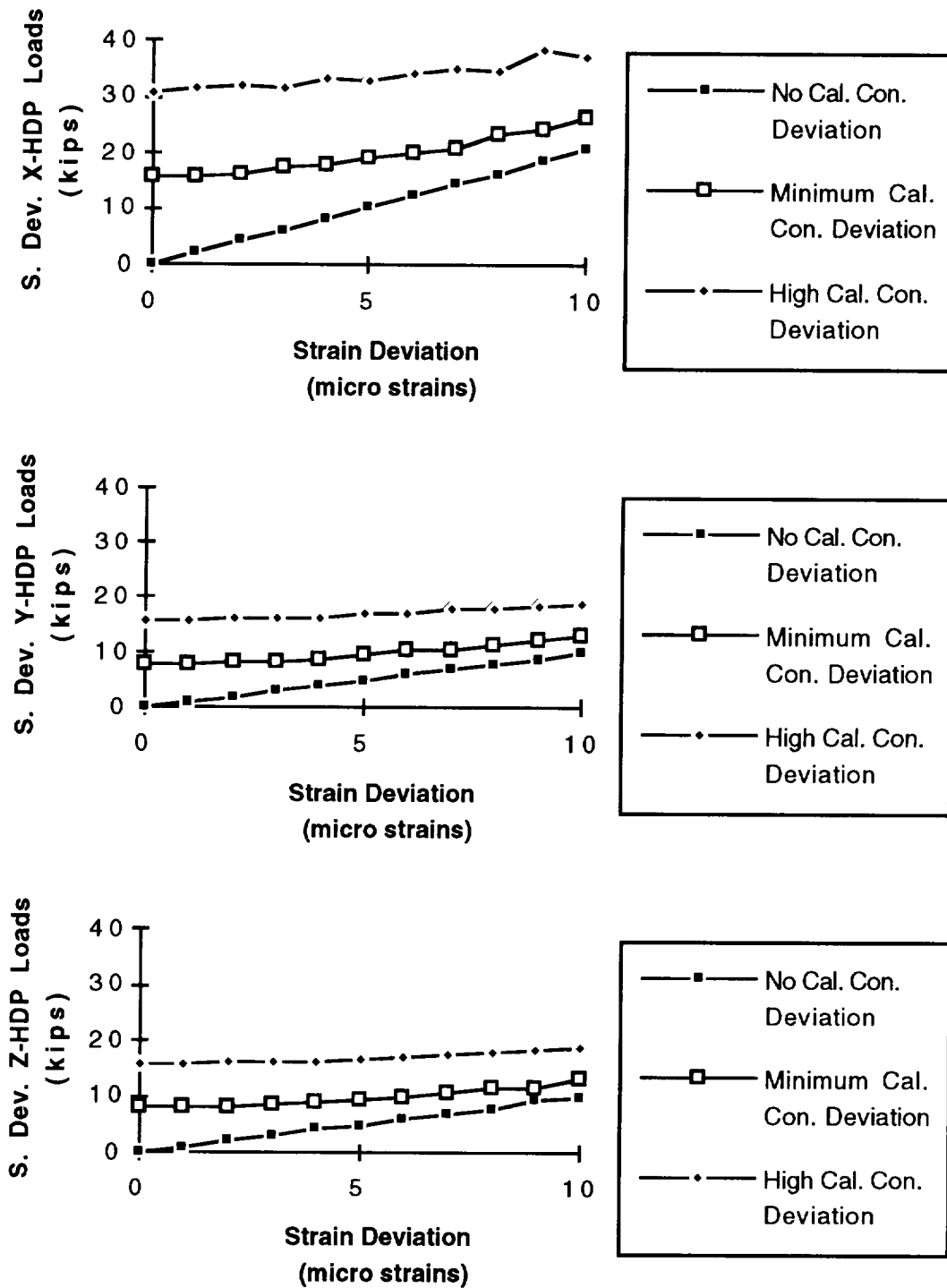
Figure 9. Effect of calibration constant deviations and strain deviations on x-, y-, and z-direction HDP load deviations.
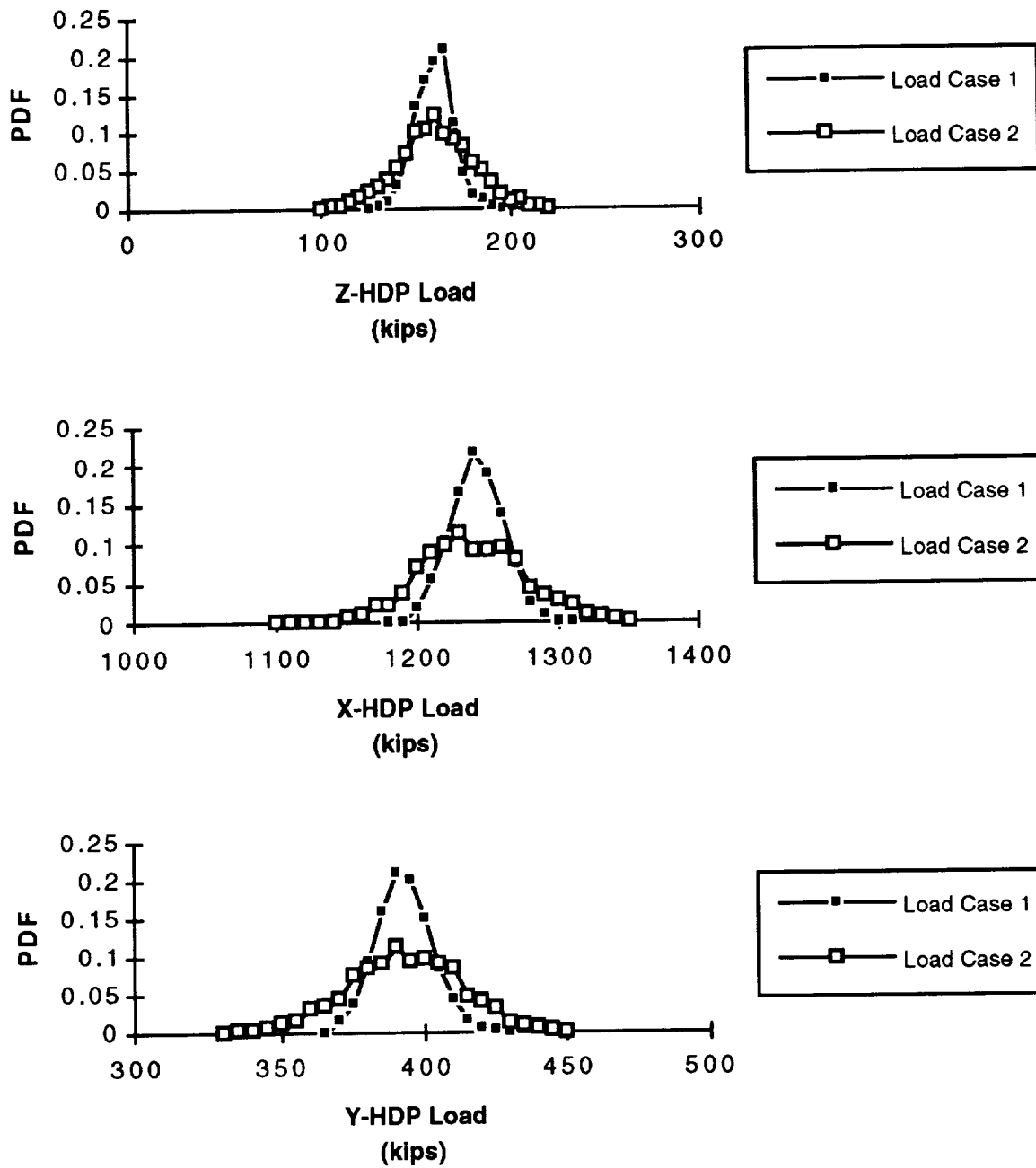
Figure 10. Distributions of HDP loads for two cases.
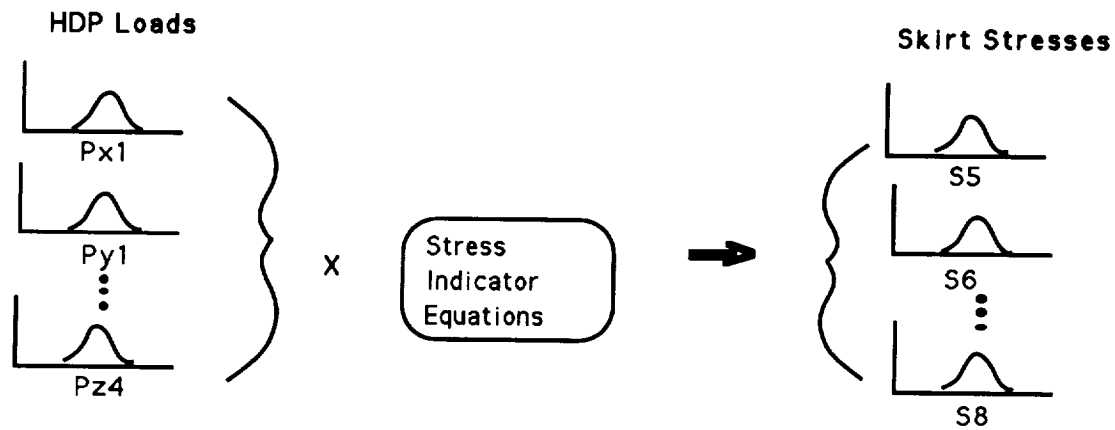
Figure 11. Procedure for calculating skirt stress distributions from HDP load distributions.
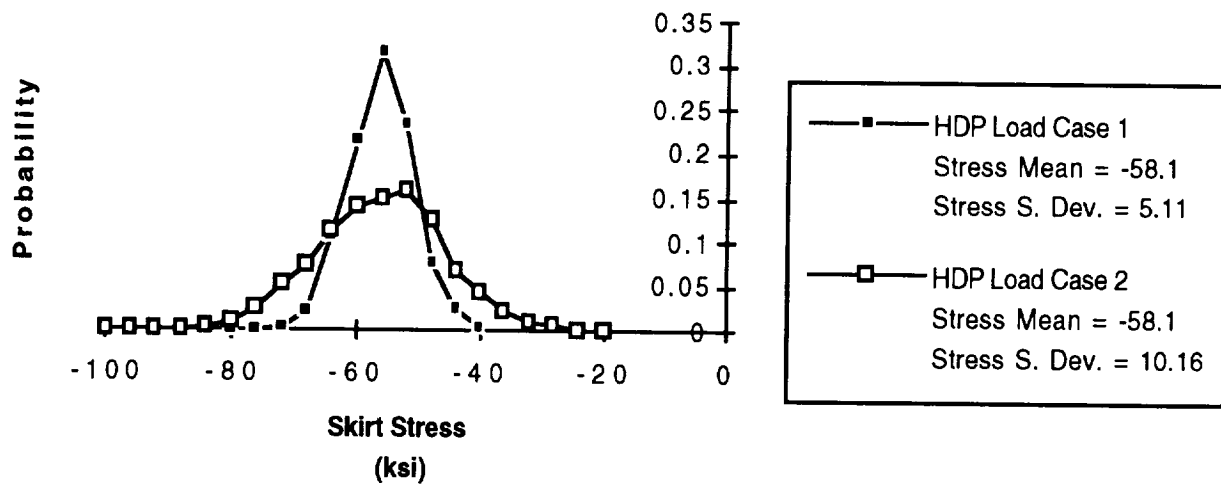
Figure 12. Skirt stress distributions for two cases of strain and calibration constant deviations.
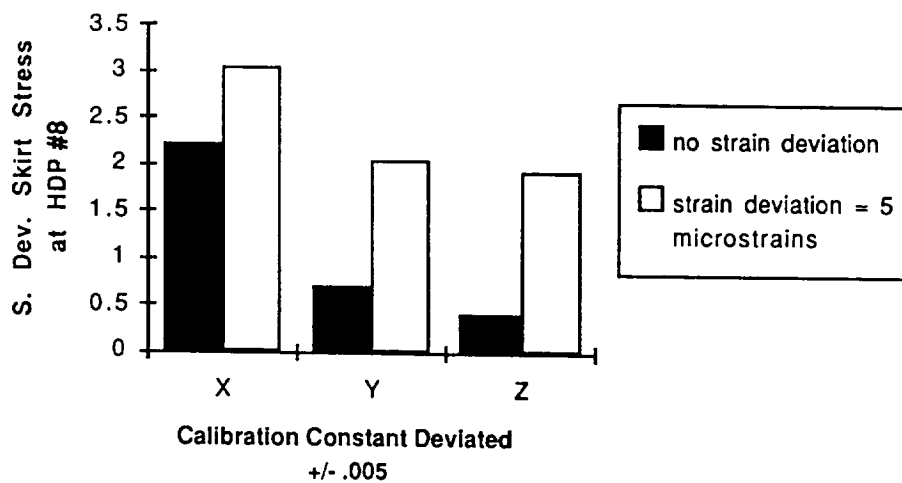
Figure 13. Relative effect of calibration constant deviations on skirt stress above HDP No. 8.

23
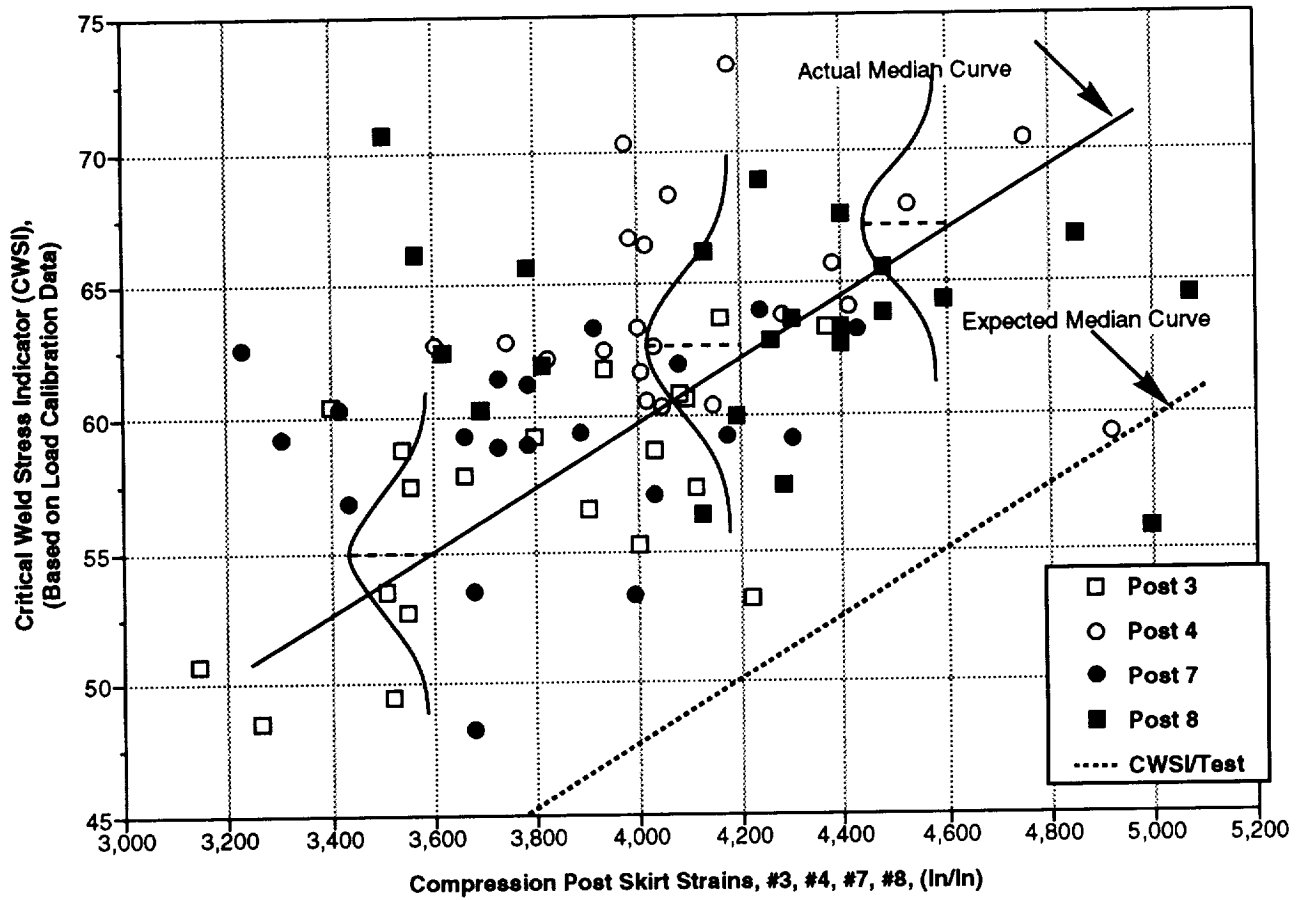
Figure 14. STS flight measured skirt strains versus CWSI based on HDP load calibration (18 flights).
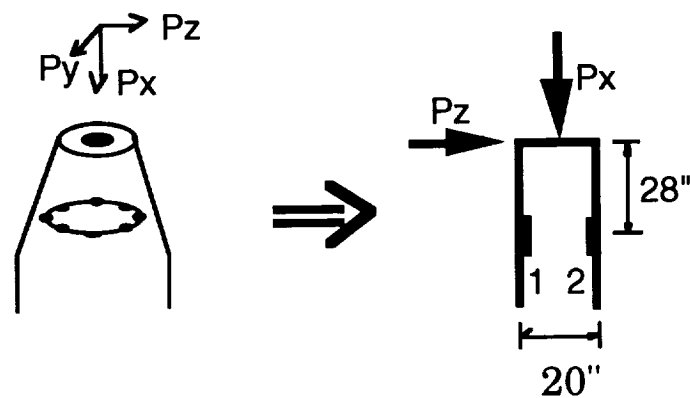

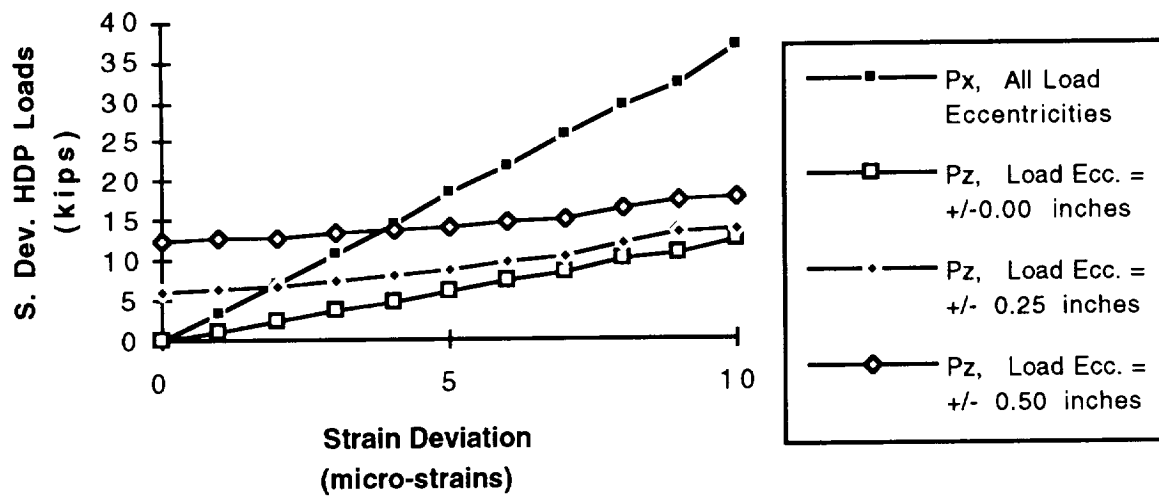Figure 15. HDP load cell modeled as simple cantilever beam.

Figure 16. Effect of load point deviations on HDP load deviations.
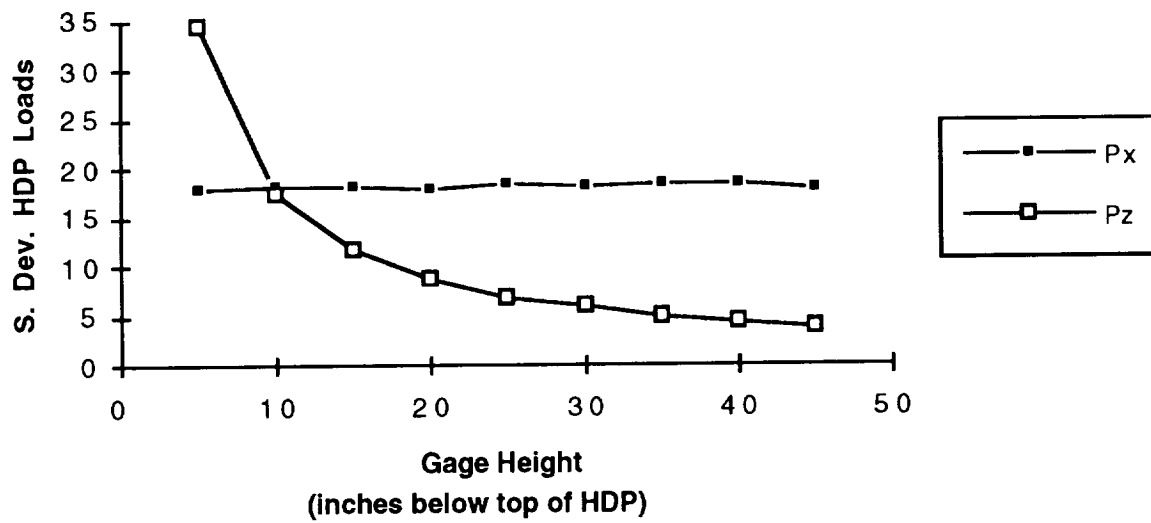

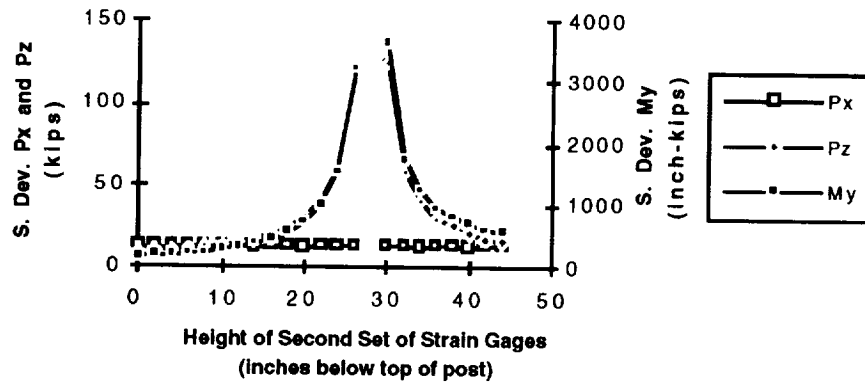Figure 17. Effect of gauge height on HDP load deviations.

Figure 18. Effect of height of second set of gauges on HDP load deviations.
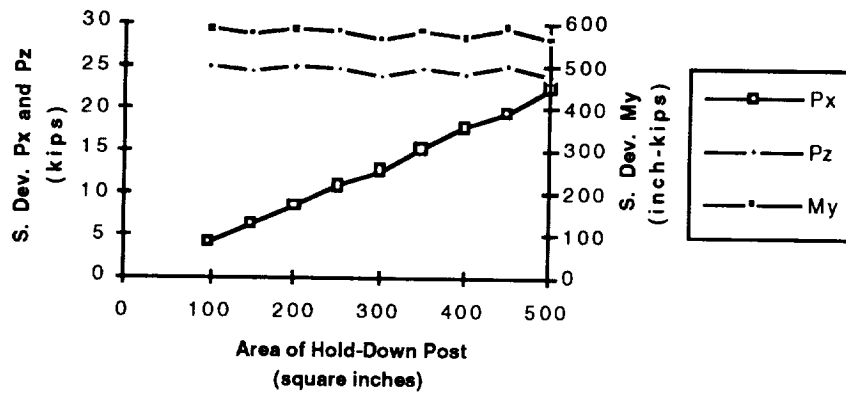Strain deviation = ±5 microstrains.

Figure 19. Effect of HDP cross-section area on HDP load deviations.
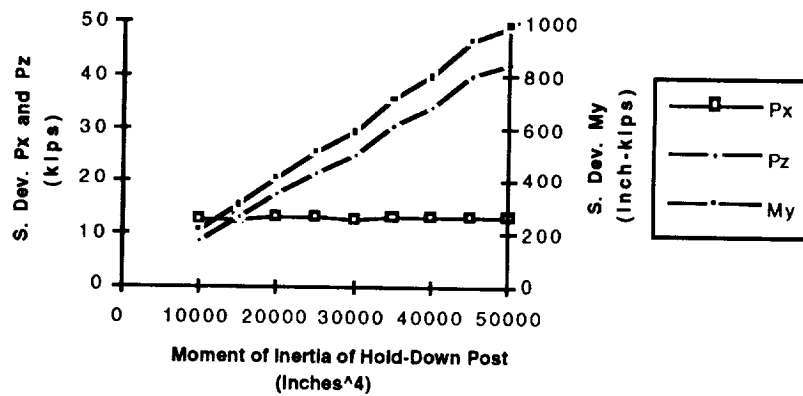Strain deviation = ±5 microstrains.

Figure 20. Effect of HDP moment of inertia on HDP load deviations.
Strain deviation = ±5 microstrains.

REPORT DOCUMENTATION PAGE

Public reporting burden for this collection of information is estimated to average 1 hour per response, including the time for reviewing instructions, searching existing data sources, gathering and maintaining the data needed, and completing and reviewing the collection of information. Send comments regarding this burden estimate or any other aspect of this collection of information, including suggestions for reducing this burden, to Washington Headquarters Services, Directorate for Information Operations and Reports, 1215 Jefferson Davis Highway, Suite 1204, Arlington, VA 22202-4302, and to the Office of Management and Budget, Paperwork Reduction Project (0704-0188), Washington, DC 20503

1. AGENCY USE ONLY (Leave blank)	2. REPORT DATE	3. REPORT TYPE AND DATES COVERED
	March 1993	Technical Paper

4. TITLE AND SUBTITLE

Characterizing the Uncertainty in Holddown Post Load Measurements

5. FUNDING NUMBERS

6. AUTHOR(S)

J.A. Richardson* and J.S. Townsend

7. PERFORMING ORGANIZATION NAME(S) AND ADDRESS(ES)

George C. Marshall Space Flight Center
Marshall Space Flight Center, Alabama 35812

8. PERFORMING ORGANIZATION REPORT NUMBER

M–715

9. SPONSORING/MONITORING AGENCY NAME(S) AND ADDRESS(ES)

National Aeronautics and Space Administration
Washington, DC 20546

10. SPONSORING/MONITORING AGENCY REPORT NUMBER

NASA TP–3332

11. SUPPLEMENTARY NOTES

Prepared by Structures and Dynamics Laboratory, Science and Engineering Directorate.
*University of Alabama, Tuscaloosa, Alabama

12a. DISTRIBUTION/AVAILABILITY STATEMENT

Unclassified—Unlimited

Subject Category: 35

12b. DISTRIBUTION CODE

13. ABSTRACT (Maximum 200 words)

In order to understand unexpectedly erratic load measurements in the launch-pad supports for the space shuttle, the sensitivities of the load cells in the supports were analyzed using simple probabilistic techniques. NASA engineers use the loads in the shuttle's supports to calculate critical stresses in the shuttle vehicle just before lift-off. The support loads are measured with "load cells" which are actually structural components of the mobile launch platform which have been instrumented with strain gauges. Although these load cells adequately measure vertical loads, the horizontal load measurements have been erratic. The load measurements were simulated in this study using Monte Carlo simulation procedures. The simulation studies showed that the support loads are sensitive to small deviations in strain and calibration. In their current configuration, the load cells will not measure loads with sufficient accuracy to reliably calculate stresses in the shuttle vehicle. A simplified model of the holddown post (HDP) load measurement system was used to study the effect on load measurement accuracy for several factors, including load point deviations, gauge heights, and HDP geometry.

14. SUBJECT TERMS Probabilistic, Load Cell, Strain Gage, Holddown Post, Monte Carlo, Loads, Space Shuttle, Uncertainty			15. NUMBER OF PAGES 36
			16. PRICE CODE A03
17. SECURITY CLASSIFICATION OF REPORT	18. SECURITY CLASSIFICATION OF THIS PAGE	19. SECURITY CLASSIFICATION OF ABSTRACT	20. LIMITATION OF ABSTRACT
Unclassified	Unclassified	Unclassified	Unlimited